Mon. Not. R. Astron. Soc. **000**, 000–000 (0000) Printed 31 October 2018 (MN LATEX style file v1.4)

Full-sky correlations of peaks in the microwave background

Alan F. Heavens and Sujata Gupta
Institute for Astronomy, University of Edinburgh, Blackford Hill, Edinburgh EH9 3HJ, U.K.

31 October 2018

ABSTRACT
We compute precise predictions for the two-point correlation function of local maxima (or minima) in the temperature of the microwave background, under the assumption that it is a random gaussian field. For a given power spectrum and peak threshold there are no adjustable parameters, and since this analysis does not make the small-angle approximation of Heavens & Sheth (1999), it is essentially complete. We find oscillatory features which are absent in the temperature autocorrelation function, and we also find that the small-angle approximation to the peak-peak correlation function is accurate to better than 0.01 on all scales. These high-precision predictions can form the basis of a sensitive test of the gaussian hypothesis with upcoming all-sky microwave background experiments MAP and Planck, affording a thorough test of the inflationary theory of the early Universe. To illustrate the effectiveness of the technique, we apply it to simulated maps of the microwave sky arising from the cosmic string model of structure formation, and compare with the bispectrum as a non-gaussian discriminant. We also show how peak statistics can be a valuable tool in assessing and statistically removing contamination of the map by foreground point sources.

Key words: cosmic background radiation - cosmology; theory - early Universe - large-scale structure of Universe.

1 INTRODUCTION

The cosmic microwave background radiation (CMB) presents an ideal opportunity to test theories of the early Universe. At the time of last scattering, the Universe is a relatively straightforward, almost uniform, mixture of photons, baryons, electrons and dark matter. The physics is well-understood, and free from the very complicated effects which make interpretation of the present-day matter distribution more complicated. The microwave background thus offers the possibility of accurately testing models of structure formation. A generic test can readily be made between two classes of structure-formation models, based on inflation and cosmic defects respectively. There are several ways to do this; the power spectrum itself is a useful discriminant of specific models. We concentrate here on a generic test: most inflationary models predict that the microwave background temperature map will be very close to a random gaussian field, whereas generically defect models predict a non-gaussian temperature map. It turns out that testing the gaussian nature of the initial fluctuations is easier through analysis of CMB fluctuations than large-scale structure (Verde et al. 2000), although tests based on number densities of high-redshift objects may also be useful (Robinson, Gawiser & Silk 2000,Matarrese, Verde & Jimenez 2000).

Current evidence from Boomerang (de Barnardis et al. 2000) and MAXIMA (Hanany et al. 2000,Balbi et al. 2000) favours inflation models, since the power spectrum is acceptable for certain combinations of cosmological parameters. Indeed, the major scientific goal of these and future experiments such as the *Microwave Anisotropy Probe* (MAP) and *Planck Surveyor* (Bersanelli et al. 1996), is to derive cosmological parameters from the power spectrum. To make this interpretation requires that the temperature map is created by inflation or some similar process, not by defects, and that the map is not seriously contaminated by foregrounds. In both of these areas, the statistics of peaks can be a valuable tool. The process is quite straightforward: given a power spectrum, the statistical properties of peaks of a gaussian field are fully determined - there are no free parameters. If the peaks are not consistent with the predictions, then either the CMB temperature map is not gaussian, or it is significantly contaminated by foregrounds, or both. In either of these cases, the derived cosmological parameters from the power spectrum will be suspect. In this paper, we compute the predictions for the correlation function of local maxima (and minima) for a gaussian field. The paper generalises the work of Heavens & Sheth (1999) in dropping the small-angle

approximation: the results of this paper can be used for all valid separations on the sky. There are several ways to test the gaussian hypothesis, such as the three-point function (e.g. Hinshaw et al. 1994, Falk, Rangarajan & Srednicki 1993, Luo & Schramm 1993, Gangui et al. 1994), the genus and Euler-Poincaré statistic (Coles 1989, Gott et al. 1990, Luo 1994b, Smoot et al. 1994), the bispectrum (Luo 1994a, Heavens 1998, Ferreira, Magueijo & Gorski 1998), studies of tensor modes in the CMB (Coulson, Crittenden & Turok 1994), excursion set properties (Barreiro et al. 1998, Barreiro, Martinez-Gonzales & Sanz 2000), peak statistics (Bond & Efstathiou 1987, Kogut et al. 1995, Kogut et al. 1996, Barreiro et al. 1997) and wavelet analyses (e.g. Mukherjee, Hobson & Lasenby 2000, Aghanim & Forni 1999, Forni & Aghanim 1999). One advantage which the method presented here has is the possibility of assessing and removing contamination by foreground point sources. We return to this in the discussion. Non-gaussian signals have been reported for the COBE map by Ferreira, Magueijo & Gorski (1998) (see also Pando, Valls-Gabaud & Fang 1998, Kamionkowski & Jaffe 1998, Bromley & Tegmark 1999, Mukherjee, Hobson & Lasenby 2000, Magueijo 2000) . If this nongaussian signal is really present in the microwave background map, and not the result of some artefact (Banday, Zaroubi & Górski 2000), then it would be a severe challenge to inflation models, as it is many orders of magnitude larger than expected (e.g. Verde et al. 2000 and references therein).

2 METHOD

In this section, we compute the two-point correlation function of local maxima in 2D gaussian random fields on the surface of a sphere. The method essentially follows that of Heavens & Sheth (1999), who used a Fourier analysis which assumed a flat sky. That analysis should be accurate for small separations; the analysis in this paper is general.

2.1 Peaks on the surface of a sphere

We define the temperature fluctuation by $\delta(\theta,\phi) \equiv T(\theta,\phi)/\bar{T} - 1$, where $\bar{T}$ is the mean temperature, and its spherical harmonic transform by

$$a_{\ell m} \equiv \int d^2\Omega\, \delta(\theta,\phi) Y_\ell^{m*}(\theta,\phi) \tag{1}$$

where $\Omega = (\theta,\phi)$. The inverse is

$$\delta(\theta,\phi) = \sum_{m=-\ell,\ell;\ \ell=0,\infty} a_{\ell m} Y_\ell^m(\theta,\phi) \tag{2}$$

If the temperature map is a random gaussian field, the statistical properties of the fluctuations are specified entirely by the power spectrum, C_ℓ, defined by

$$\langle a_{\ell m} a^*_{\ell' m'} \rangle = C_\ell \delta^K_{\ell\ell'} \delta^K_{mm'} \tag{3}$$

where angle brackets indicate ensemble averages, and δ^K is a Kronecker delta function. The autocorrelation function of the temperature for points at (θ,ϕ), (θ',ϕ'), separated by an angle ψ is

$$F(x) = \langle \delta(\theta,\phi)\delta(\theta',\phi') \rangle = \sum_\ell C_\ell \left(\frac{2\ell+1}{4\pi} \right) P_\ell(x) \tag{4}$$

where $x = \cos\psi$ and P_ℓ is a Legendre polynomial. The remainder of the calculation of the peak-peak correlation function follows the method outlined in Heavens & Sheth (1999). We compute the 12×12 covariance matrix $M_{ij} = \langle v_i v_j \rangle$, where $v_i = (\mathbf{v}_1, \mathbf{v}_2)$ and the vectors $\mathbf{v}$ specify the field and its derivatives at the two points: $\mathbf{v} = (\delta, \delta_\phi, \delta_\theta, \delta_{\phi\phi}, \delta_{\phi\theta}, \delta_{\theta\theta})$. Note that $\delta_\phi \equiv \partial\delta/\partial\phi$ etc. We show how to compute the components of the covariance matrix by an example, from which the others can be readily generalised. Consider the correlation of derivatives in the ϕ direction at two points (1) and (2):

$$\langle \delta^{(1)}_\phi \delta^{(2)*}_\phi \rangle = \sum_{\ell,m} \sum_{\ell',m'} \langle a_{\ell m} a^*_{\ell' m'} \rangle \frac{\partial}{\partial\phi_1} Y_\ell^m(\theta_1,\phi_1) \frac{\partial}{\partial\phi_2} Y_{\ell'}^{m'*}(\theta_2,\phi_2) \tag{5}$$

We take the derivatives outside the summation, use the orthogonality of the $a_{\ell m}$ (3), and use the addition theorem for spherical harmonics:

$$\sum_m Y_\ell^m(\theta_1,\phi_1) Y_\ell^{m*}(\theta_2,\phi_2) = \frac{2\ell+1}{4\pi} P_\ell(x). \tag{6}$$

This yields

$$\langle \delta^{(1)}_\phi \delta^{(2)*}_\phi \rangle = \frac{\partial^2}{\partial\phi_1 \partial\phi_2} \sum_\ell \frac{2\ell+1}{4\pi} C_\ell P_\ell(x). \tag{7}$$

Writing $x = \cos\theta_1\cos\theta_2 + \sin\theta_1\sin\theta_2\cos(\phi_1-\phi_2)$ we can differentiate to compute the covariance matrix element. This is aided by noting that these functions are independent of the absolute positions or orientations of the two points on the sphere, depending only on their separation. We can therefore simplify the algebra by taking $\theta_1 = \theta_2 = \pi/2$, $\phi_1 = 0$, and $\phi_2 = \phi$. This element simplifies to

$$\langle \delta_\phi^{(1)} \delta_\phi^{(2)*} \rangle = \sum_\ell \frac{2\ell+1}{4\pi} C_\ell \left[\frac{dP_\ell(x)}{dx}\cos\phi - \frac{d^2P_\ell(x)}{dx^2}\sin^2\phi \right]. \tag{8}$$

Other elements are readily obtained by similar methods using Mathematica.

We invert M to get the joint probability distribution for the 12 variables,

$$p(\mathbf{v}_1,\mathbf{v}_2) = \frac{1}{(2\pi)^6||M||^{1/2}} \exp\left(-\frac{1}{2}v_i M_{ij}^{-1} v_j\right). \tag{9}$$

and integrate subject to constraints that the two points are maxima:

$$\begin{aligned} 1+\xi(r|\nu_1,\nu_2) &= \frac{1}{4\theta_*^4 n_{pk}(\nu_1) n_{pk}(\nu_2)} \int_{X_1=0}^{\infty}\int_{X_2=0}^{\infty}\int_{Y_1=-X_1}^{X_1}\int_{Y_2=-X_2}^{X_2}\int_{Z_1=-\sqrt{X_1^2-Y_1^2}}^{\sqrt{X_1^2-Y_1^2}}\int_{Z_2=-\sqrt{X_2^2-Y_2^2}}^{\sqrt{X_2^2-Y_2^2}} dX_1 dX_2 dY_1 dY_2 dZ_1 dZ_2 \\ &\times \left(X_1^2-Y_1^2-Z_1^2\right)\left(X_2^2-Y_2^2-Z_2^2\right) p(\nu_1, X_1, Y_1, Z_1, \eta^{(1)}_{\phi,\theta}=0, \nu_2, X_2, Y_2, Z_2, \eta^{(2)}_{\phi,\theta}=0). \end{aligned} \tag{10}$$

where $n_{pk}(\nu)d\nu$ is the number density of peaks between height ν and $\nu+d\nu$, given by A1.9 of Bond & Efstathiou (1987). By symmetry, (10) is also the correlation function of minima at $-\nu_1$, $-\nu_2$. We have defined the symbols

$$\begin{aligned} \nu &\equiv \frac{\delta}{\sigma_0} \\ \eta_\phi &\equiv \frac{\delta_\phi}{\sigma_1} \\ \eta_\theta &\equiv \frac{\delta_\theta}{\sigma_1} \\ X &\equiv -\frac{(\delta_{\phi\phi}+\delta_{\theta\theta})}{\sigma_2} \\ Y &\equiv \frac{(\delta_{\phi\phi}-\delta_{\theta\theta})}{\sigma_2} \\ Z &\equiv \frac{2\delta_{\phi\theta}}{\sigma_2} \end{aligned} \tag{11}$$

and the moments of the power spectrum are defined by

$$\begin{aligned} \sigma_0^2 &\equiv F(1) \\ \sigma_1^2 &\equiv 2F'(1) \\ \sigma_2^2 &\equiv 4\left[F'(1)+2F''(1)\right] \end{aligned} \tag{12}$$

where $F'(1) = dF(x)/dx|_{x=1}$ etc. We also define the spectral parameters

$$\gamma \equiv \sigma_1^2/(\sigma_0\sigma_2) \qquad \theta_* \equiv \sqrt{2}\frac{\sigma_1}{\sigma_2}. \tag{13}$$

These allow simplification of the covariance matrix, with variables in the order $(\nu_1, \eta_{\phi1}, X_1, Y_1, \nu_2, \eta_{\phi2}, X_2, Y_2, \eta_{\theta1}, Z_1, \eta_{\theta2}, Z_2)$, to the block form

$$M_{ij} = \begin{pmatrix} A & B & 0 \\ B^T & A & 0 \\ 0 & 0 & C \end{pmatrix} \tag{14}$$

where

$$A = \begin{pmatrix} 1 & \gamma & 0 & 0 \\ \gamma & 1 & 0 & 0 \\ 0 & 0 & \frac{1}{2} & 0 \\ 0 & 0 & 0 & (1-\theta_*^2)/2 \end{pmatrix}. \tag{15}$$

Defining $h(x) \equiv F(x)/\sigma_0^2$, $S \equiv \sin\phi$ and $C \equiv \cos\phi$,

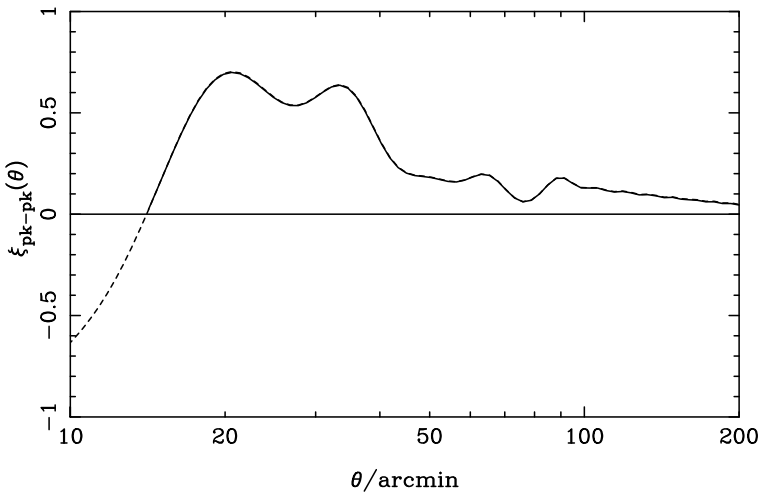

Figure 1. (Solid line) The correlation function for peaks above a $+1\sigma$ threshold, in a mixed dark matter model with CDM, vacuum and baryon density parameters $\Omega_{CDM} = 0.8$, $\Omega_\nu = 0.15$ and $\Omega_B = 0.05$. Hubble constant is $H_0 = 60$ km s^{-1} Mpc^{-1}. For comparison, the flat sky results of Heavens & Sheth (1999) are shown dotted. The results coincide to an accuracy of better than 0.004.

$$B = \begin{pmatrix} h & \frac{\theta_*^2\left(2\,C\,h' - S^2\,h''\right)}{2\,\gamma} & -\frac{S\,\theta_*\,h'}{\sqrt{2}\,\gamma} & \frac{S^2\,\theta_*^2\,h''}{2\,\gamma} \\ B_{21} & \frac{\theta_*^4\left[4\,C\,h' + \left(8\,C^2 - 6\,S^2\right)h'' - 8\,C\,S^2\,h^{(3)} + S^4\,h^{(4)}\right]}{4\,\gamma^2} & \frac{S\,\theta_*^3\left(-2\,h' - 4\,C\,h'' + S^2\,h^{(3)}\right)}{2\sqrt{2}\,\gamma^2} & \frac{\theta_*^4\left(6\,S^2\,h'' + 6\,C\,S^2\,h^{(3)} - S^4\,h^{(4)}\right)}{4\,\gamma^2} \\ -B_{13} & -B_{23} & \frac{\theta_*^2\left(C\,h' - S^2\,h''\right)}{2\,\gamma^2} & \frac{S\,\theta_*^3\left(-2\,C\,h'' + S^2\,h^{(3)}\right)}{2\sqrt{2}\,\gamma^2} \\ B_{14} & B_{24} & -B_{34} & \frac{\theta_*^4\left[2\left(1+C^2\right)h'' - 4\,C\,S^2\,h^{(3)} + S^4\,h^{(4)}\right]}{4\,\gamma^2} \end{pmatrix} \quad (16)$$

where $h^{(3)}(x) \equiv h'''(x)$ etc, and we write the lower triangle in terms of the upper triangular matrix for conciseness. Finally,

$$C = \begin{pmatrix} \frac{1}{2} & \frac{\theta_*^2\,h'}{2\,\gamma^2} & 0 & -\frac{S\,\theta_*^3\,h''}{\sqrt{2}\,\gamma^2} \\ \frac{\theta_*^2\,h'}{2\,\gamma^2} & \frac{1}{2} & \frac{S\,\theta_*^3\,h''}{\sqrt{2}\,\gamma^2} & 0 \\ 0 & \frac{S\,\theta_*^3\,h''}{\sqrt{2}\,\gamma^2} & \frac{1-\theta_*^2}{2} & \frac{\theta_*^4\left(C\,h'' - S^2\,h^{(3)}\right)}{\gamma^2} \\ -\frac{S\,\theta_*^3\,h''}{\sqrt{2}\,\gamma^2} & 0 & \frac{\theta_*^4\left(C\,h'' - S^2\,h^{(3)}\right)}{\gamma^2} & \frac{1-\theta_*^2}{2} \end{pmatrix} \quad (17)$$

The correlation function for peaks above a certain threshold ν is obtained by adding two further integrations over ν_1 and ν_2, and replacing the differential number densities $n_{pk}(\nu)$ in the denominator of (10) by numerically-evaluated integrals $n_{pk}(>\nu)$. For peaks above a threshold, the 8D integration can be reduced to 6, as the integrals over ν_2 and z_2 can be done analytically. Very accurate integrations can then be done on a desktop workstation in about 50 seconds.

3 RESULTS

We run CMBFAST (Seljak & Zaldarriaga 1996) to generate the power spectrum C_ℓ, and model the beam with a gaussian of FWHM b, so multiply the power spectrum by a gaussian $\exp\left[-\sigma^2\ell(\ell+1)\right]$, with $\sigma = b/\sqrt{8\ln 2}$. We have not included the effects of gravitational lensing on the temperature field. As shown by Takada, Komatsu & Futamase (2000), the effect is small except for separations up to the first peak, where the anticorrelation is reduced in magnitude. Figs. 1 and 2 show the correlation function of peaks above a 1σ threshold for a mixed dark matter model, along with the results of the flat-sky calculation of Heavens & Sheth (1999). The differences are at the level of ~ 0.005.

4 CORRELATION FUNCTION VS BISPECTRUM FOR STRING MAPS

There are many methods for testing the gaussian hypothesis, and it is tempting to ask which is the best. Unfortunately the question is badly posed, as methods will fare differently depending on the exact properties of the non-gaussian field considered. Here we focus on one particular non-gaussian field, produced by a network of cosmic strings. Fig. 3 shows a realisation of the temperature map expected from cosmic strings, one of two kindly provided by Francois Bouchet. The lensing effect of the moving strings is added to a gaussian background map, approximately as expected from the string model (Pen, Seljak &

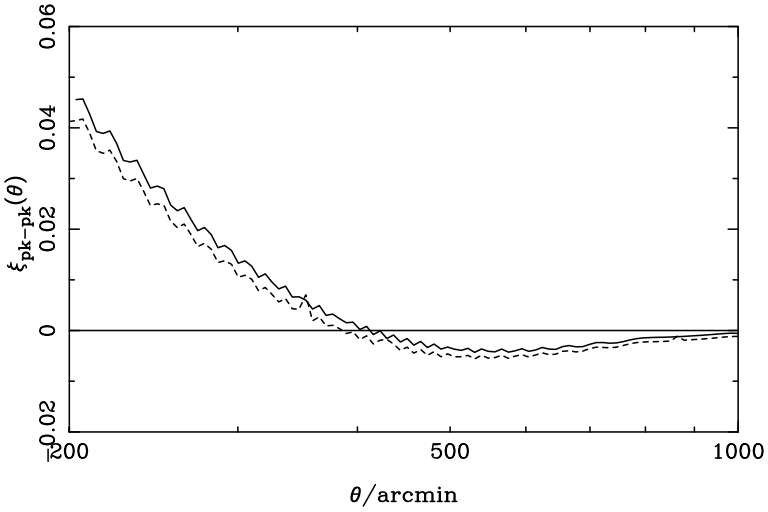

Figure 2. As Fig. 1, but at larger angle separations between 3.3 and 16.7 degrees.

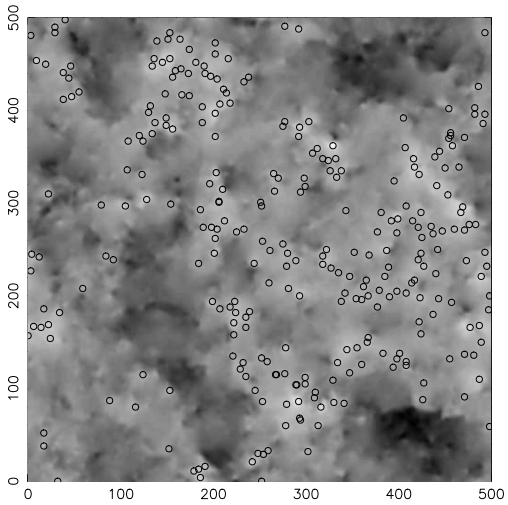

Figure 3. Simulated sky map for cosmic strings, consisting of a gaussian background, with the lensing effect of a string network superimposed. Peaks above 1σ are circled.

Turok 1997) (see also Simatos & Perivolaropoulos 2000, Avelino & Martins 2000). We consider two diagnostics: the peak-peak correlation function, and the bispectrum (e.g. Heavens 1998, Ferreira, Magueijo & Gorski 1998, Gangui & Martin 2000). The string maps we have are 12.5° on a side, and we would expect the bispectrum to have difficulty in distinguishing these maps from gaussian maps with the same power spectrum (Luo 1994a). The interesting question is whether the peak correlation function can do better. Since the string simulations are performed on a small, flat patch of sky, we use a Fourier transform, to compute the flat-sky bispectrum from the Fourier coefficients $\delta(\mathbf{k}) \equiv \int \mathbf{d^2x}\delta(\mathbf{x})\exp(\mathbf{ik}.\mathbf{x})$:

$$\langle\delta(\mathbf{k}_1)\delta(\mathbf{k}_2)\delta(\mathbf{k}_3)\rangle = (2\pi)^2 B(\mathbf{k}_1,\mathbf{k}_2,\mathbf{k}_3)\delta^D(\mathbf{k}_1+\mathbf{k}_2+\mathbf{k}_3) \tag{18}$$

The angle brackets indicate ensemble averages, and δ^D is the Dirac delta function. For a gaussian field the bispectrum is zero, and for all fields the bispectrum is zero unless $\mathbf{k}_1+\mathbf{k}_2+\mathbf{k}_3 = \mathbf{0}$. Following the work of Matarrese, Verde & Heavens (1997) and Verde et al. (1998) in large-scale structure, we consider two configurations of triangles: equilaterals, and zero-area triangles with two equal wavevectors and one of twice the size. The bispectrum is real, but the $\delta(\mathbf{k})$ are not, so we consider the estimate

$$D_\alpha = \langle Re(\delta(\mathbf{k}_1)\delta(\mathbf{k}_2)\delta(\mathbf{k}_3))\rangle \tag{19}$$

and average over thin shells in $k-$space.

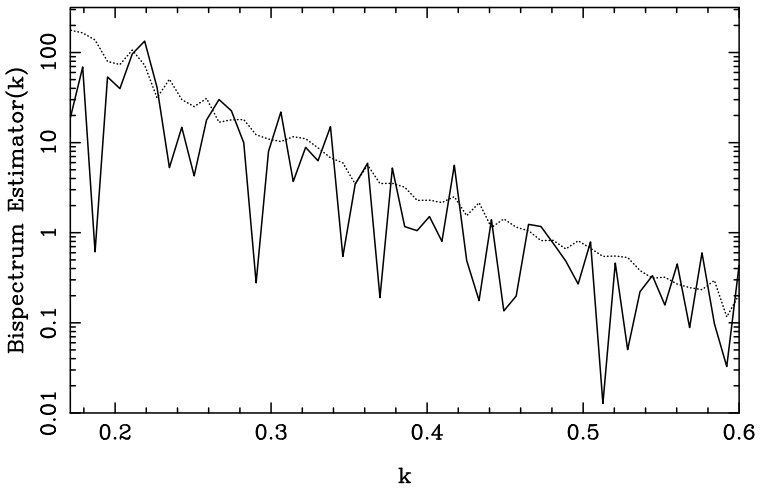

Figure 4. The equilateral bispectrum as estimated from map with string foreground and gaussian temperature on last-scattering surface (solid), and cosmic r.m.s. (dotted).

	equilateral	zero-area	$\sqrt{2/(n-1)}$
Map 1	1.06	0.96	0.19
Map 2	1.29	1.42	0.19

Table 1. Reduced χ-squared values of the deviation of the bispectra from a gaussian model of the two modified maps, consisting of intrinsic gaussian and cosmic string generated fluctuations. The r.m.s. of the reduced χ^2 for a gaussian model with $n = 55$ data is shown in the final column.

Fig. 4 displays the equilateral estimated bispectrum for the string map shown in Fig. 3. Also shown is the cosmic r.m.s. for a gaussian field of the same power spectrum, $\langle|\delta_{\mathbf{k}}|^2\rangle^{3/2}$. We show in Table 1 reduced χ^2 values for both equilateral triangles and zero-area triangles for the two simulated maps. With 55 bins, the variance in the reduced χ^2 for a gaussian field is shown in the final column. We find no significant departure from gaussianity with this test.

Fig. 5 shows the correlation function of peaks above 1σ (where σ^2 is the map variance) for the map shown in Fig. 3. The map is smoothed with a gaussian beam of FWHM $5.5'$ to model the Planck beam. The errors for the peak-peak correlation

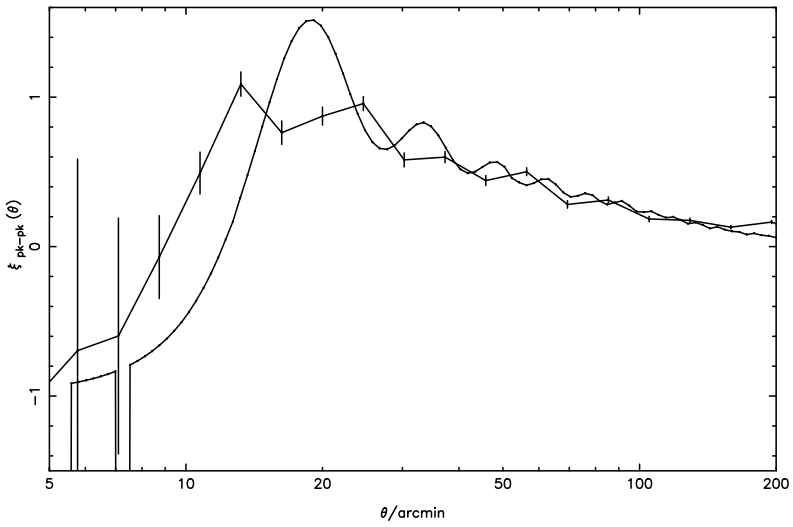

Figure 5. The correlation function of peaks above 1σ calculated from the map of Fig. 3. Errors are Poisson, and hence underestimates. Superimposed is the correlation function from a gaussian map with the same power spectrum. Note the excess of string peaks around 10-15 arcminutes.

function are Poisson errors, which will be underestimates. However, it is clear that the peak correlation function of the string map is significantly different from that of a gaussian map with the same power spectrum. The most striking difference is the presence of peaks in the string map which are separated by $10 - 20$ arcminutes. These appear in greater numbers than in the gaussian map, and this could be the most obvious manifestation of strings.

5 DISCUSSION

We have presented calculations of the exact correlation function of peaks in a random gaussian field defined on the surface of a sphere. No small-angle approximation is made, so the method is an advance on the flat-sky computations of Heavens & Sheth (1999) and now effectively complete. The formalism allows very accurate theoretical predictions of the peak-peak correlation function for temperature fluctuations in the microwave background, which is the application considered here. We envisage the main use of this method being as a sensitive test of the gaussian hypothesis. Since inflationary models generically predict a temperature field which is very close to gaussian, this is a consistency test for inflation. Other structure formation models, based for example on strings, predict non-gaussian temperature maps. Although the visual appearance of string maps is evidently non-gaussian, it is not necessarily easy to find statistics which will unambiguously distinguish them from gaussian fields. To illustrate this point, we have analysed 12.5-degree square simulated maps of string models, using the bispectrum and the peak-peak correlation function as distinguishing statistics. We find that, while cosmic variance in the bispectrum makes it difficult to use on a small patch of sky, the peak-peak correlation function clearly rules out a gaussian map.

In practice, maps of the microwave background will be contaminated at some level by point sources, amongst other things. Peak statistics may be useful in assessing this contribution. The most straightforward example is that an uncontaminated map has the same average number density of maxima and minima; a significant excess of maxima would be indicative of contamination. Unfortunately the theory of peaks is not able to tell us the *distribution* of the number of maxima or minima within a finite sky (only its mean), but it is a straightforward matter to determine the distribution by monte carlo realisations. One can attempt to go further than this, by removing statistically the contribution from the point sources, provided one knows from other observations what their correlation function is. Assuming the point sources are uncorrelated with the microwave background peaks, the correlation function of the combined map is simply a weighted mean of the two. The point sources will contribute to the power spectrum; one can vary the assumed contribution from point sources and modify the power spectrum and the derived microwave background peak correlation function accordingly. If consistency can be achieved, one will be confident both of the gaussian nature of the microwave background, and the level of point source contamination.

Acknowledgments

We are grateful to Francois Bouchet for providing the simulated catalogues, and to Ravi Sheth for useful discussions. Computations were made partly using Starlink facilities.

REFERENCES

Aghanim N., Forni O., 1999. A& A, 347, 409.
Avelino P. P., Martins C. J. A. P., 2000. Phys. Rev. Lett., 85, 1370.
Balbi A., Ade P., Bock J., Borrill J., Boscaleri A., de Bernardis P., Ferreira P. G., Hanany S., Hristov V. V., Jaffe A. H., Lee A. T., Oh S., Pascale E., Rabii B., Richards P. L., Smoot G. F., Stompor R., Winant C. D., Wu J. H. P., 2000. ApJ(Lett), in press.
Banday A. J., Zaroubi S., Górski K. M., 2000. ApJ, 533, 575.
Barreiro R., Sanz J., Martinez-Gonzales E., Cayon L., J.Silk, 1997. ApJ, 478, 1.
Barreiro R., Sanz J., Martinez-Gonzales E., J.Silk, 1998. MNRAS, 296, 693.
Barreiro R., Martinez-Gonzales E., Sanz J., 2000. astro-ph, 0009365.
Bersanelli M., Bouchet F., Griffin M., Lamarre J., Mandolesi N., Norgaard-Nielsen H., Pace O., Polny J., Puget J., Tauber J., Vittorio N., Volonté S., 1996. ESA D/SCI, 96, 3.
Bond J. R., Efstathiou G. P., 1987. MNRAS, 226, 655.
Bromley B., Tegmark M., 1999. ApJ(Lett), 524, 79.
Coles P., 1989. MNRAS, 234, 509.
Coulson D., Crittenden R., Turok N., 1994. Phys. Rev. Lett., 73, 2390.
de Barnardis et al. P., 2000. Nat, 404, 955.
Falk T., Rangarajan R., Srednicki M., 1993. ApJ(Lett), 403, 1.
Ferreira P., Magueijo J., Gorski K., 1998. ApJ(Lett), 503, 1.
Forni O., Aghanim N., 1999. A& AS, 137, 553.
Gangui A., Martin J., 2000. MNRAS, 313, 323.
Gangui A., Lucchin F., Matarrese S., Mollerach S., 1994. ApJ, 430, 447.

Gott J. R., Park C., Juszkiewicz R., Bies W., Bennett D., Bouchet F., Stebbins A., 1990. ApJ, 352, 1.
Hanany S., Ade P., Balbi A., Bock J., Borrill J., Boscaleri A., de Bernardis P., Ferreira P. G., Hristov V. V., Jaffe A. H., Lange A. E., Lee A. T., Mauskopf P. D., Netterfield C. B., Oh S., Pascale E., Rabii B., Richards P. L., Smoot G. F., Stompor R., Winant C. D., Wu J. H. P., 2000. ApJ(Lett), in press.
Heavens A. F., Sheth R. K., 1999. MNRAS, 310, 1062.
Heavens A. F., 1998. MNRAS, 299, 805.
Hinshaw G., Kogut A., Gorski K., Banday A., Bennett C., Lineweaver C., Lubin P., Smoot G., Wright E., 1994. ApJ, 431, 1.
Kamionkowski M., Jaffe A., 1998. Nat, 395, 639.
Kogut A., Banday A., Bennett C., Hinshaw G., Lubin P., Smoot G., 1995. ApJ, 439, L29.
Kogut A., Banday A., Bennett C., Gorski K., Hinshaw G., Smoot G., Wright E., 1996. ApJ, 464, L29.
Luo X., Schramm D., 1993. Phys. Rev. Lett., 71, 1124.
Luo X., 1994a. ApJ(Lett), 427, 71.
Luo X., 1994b. Phys. Rev., D49, 3810.
Magueijo J., 2000. ApJ(Lett), 528, 57.
Matarrese S., Verde L., Heavens A., 1997. MNRAS, 290, 651.
Matarrese S., Verde L., Jimenez R., 2000. MNRAS, in press.
Mukherjee P., Hobson M. P., Lasenby A. N., 2000. astro-ph, /0001385.
Pando J., Valls-Gabaud D., Fang L., 1998. Phys. Rev. Lett., 79, 1611.
Pen U.-L., Seljak U., Turok N., 1997. Phys. Rev. Lett., 79, 1611.
Robinson J., Gawiser E., Silk J., 2000. ApJ, 532, 1.
Seljak U., Zaldarriaga M., 1996. ApJ, 469, 437.
Simatos N., Perivolaropoulos L., 2000. astro-ph, 0009294.
Smoot G. F., Tenorio L., Banday A., Kogut A., Wright E. L., Hinshaw G., Bennett C. L., 1994. ApJ, 437, 1.
Takada M., Komatsu E., Futamase T., 2000. ApJ(Lett), 533, 83.
Verde L., Heavens A., Matarrese S., Moscardini L., 1998. MNRAS, 300, 747.
Verde L., Wang L., Heavens A., Kamionkowski M., 2000. MNRAS, 313, 141.